Self-consistent modelling of glow discharges

K. Kutasi[1], P. Hartmann[2] and Z Donkó[3]

Research Institute for Solid State Physics and Optics of the Hungarian Academy of Sciences, POB 49, H-1525 Budapest, Hungary

E-mail: [1]kutasi@sunserv.kfki.hu, [2]hartmann@sunserv.kfki.hu, [3]donko@sunserv.kfki.hu

Abstract
The paper presents a self-consistent discharge model of gas discharges, the hybrid model. The applicability of the model is illustrated on a helium gas discharge. With the hybrid model the role of molecular ions in helium glow discharges is investigated. Because of the uncertainties in the determination of the electron temperature the effect of kT_e (used as an input parameter of the model) on the calculated discharge characteristics is investigated.
Keywords: *dc glow discharges, hybrid models*

1 Introduction

Low temperature, cold-cathode glow discharges are used in various application fields: in the semiconductor industry for plasma etching and deposition, for lighting and laser purposes, for plasma display panels, in analytical chemistry as spectroscopic sources for the analysis of solid materials, etc. In order to optimize these applications, a good insight into the glow discharge processes is desirable. Numerical modelling proved to be a powerful technique for this purpose.

Glow discharges are composed of many regions, which have very different emission light intensity, electric field and charge density distributions. The most important part of the glow discharges is the cathode region with the cathode sheath and the negative glow. In this region are created the charges which are necessary for the self-sustainment of the discharge. Many applications use the cathode region because of the strong light emission characteristic to the negative glow and also because of the

presence of high energy electrons and consequently of active radicals. Further in our work we talk about glow discharges which contains only the cathode sheath and the negative glow region.

In this paper, the basics of hybrid model are described and the applicability of hybrid modelling is illustrated on a helium gas discharge.

2   Hybrid model

Hybrid models consist of a fluid model and a Monte Carlo model. The fluid model makes it possible to describe the motion of charges which are in hydrodynamic equilibrium with the electric field in the low electric field region (negative glow). With the Monte Carlo model the electrons which move in the high electric field present in the cathode vicinity can be traced. The fluid models are based on a two-component fluid description of the plasma. The self-consistency is achieved by solving the Poisson equation together with the continuity (Eq. 1) and momentum transfer equations (Eq. 2) for fluid species (positive ions and electrons):

$$\frac{\partial n_e}{\partial t} + \nabla(n_e\mathbf{v}_e) = S_e, \ \frac{\partial n_i}{\partial t} + \nabla(n_i\mathbf{v}_i) = S_i, \ \triangle V = -\frac{e}{\epsilon_0}(n_i - n_e), \tag{1}$$

where $\mathbf{v}_e$ and $\mathbf{v}_i$ are the mean velocities, S_e and S_i are the source functions, n_e and n_i are the densities of electrons and ions, respectively, e is the elementary charge, V is the electric potential and ϵ_0 is the permittivity of free space. The mean velocities $\mathbf{v}_e$ and $\mathbf{v}_i$ are calculated from the momentum transfer equations for electrons and ions:

$$\Phi_e = n_e\mathbf{v}_e = -n_e\mu_e\mathbf{E} - \nabla(n_eD_e), \ \Phi_i = n_i\mathbf{v}_i = n_i\mu_i\mathbf{E} - \nabla(n_iD_i), \tag{2}$$

where $\mu_{e(i)}$ and $D_{e(i)}$ are the mobility and diffusion coefficients of electrons (ions) and $\Phi_{e(i)}$ are the corresponding fluxes. The set of fluid equations is closed by the equation describing the production of primary electrons at the cathode $j_c^- = \gamma j_c^+$, where γ is the secondary electron emission coefficient and j_c^+ and j_c^- are the ion and electron current at the cathode, respectively. The source functions of the fluid species are calculated in the Monte Carlo routine for fast electrons, which are traced in a potential distribution obtained from the fluid model (Surendra et al., 1990; Fiala et al., 1994; Donkó et al., 1998).

In the MC algorithm random numbers are used to determine the positions and the types of the collisions. The random numbers (R_{01}) have a uniform distribution in the [0,1) interval. The primary electrons emitted from the cathode and their secondaries produced in ionizing collisions are traced until they are absorbed by the anode or, due to their energy losses in inelastic collisions, they are no longer capable of producing any additional ions. The $\mathbf{r}(t)$ trajectory of electrons between successive collisions is followed by direct integration of their equation of motion:

$$m\frac{\mathrm{d}^2\mathbf{r}}{\mathrm{d}t^2} = e\mathbf{E}, \tag{3}$$

where e and m are the electron charge and mass, respectively and $\mathbf{E}$ is the electric field. The free path of electrons is assigned randomly and the position of the collision is calculated from (Boeuf et al., 1982):

$$\int_{s_0}^{s_1} n\sigma[\varepsilon(s)]\mathrm{d}s = -\ln(1 - R_{01}), \qquad (4)$$

where s_0 is the position of the last collision and s_1 is the position of the next collision measured on the curvilinear abscissa s, n is the background gas density, σ is the sum of cross sections of all possible elementary processes, ε is the kinetic energy of the electron.

The type of the collision which occurs after the free flight is chosen randomly, taking into account the values of cross sections of different processes at the energy of the colliding electron. The source function of ions S_i is accumulated from the individual ionization processes. The electrons are transferred to the slow electron group when their (kinetic+potential) energy falls below the ionization potential of the gas atoms. Here the potential energy is considered to be the difference between the maximum value of the potential in the discharge and the potential at the actual position of the electron. In the hybrid model the Monte Carlo and fluid models are solved iteratively until the stationary state of the discharges is reached.

3 Modelling of helium glow discharges

3.1 Description of the self-consistent model

It is well known that in helium glow discharges at high pressures ≥ 100 mbar high density of molecular ions are present in the discharge and are responsible for the strong UV and VUV radiation. At low pressures (several mbar) the molecular ions have been investigated only in positive column discharges. At pressures higher than 10 mbar in positive column discharges molecular ions become the dominant ions (Ichikawa et al., 1980). The aim of our work is to investigate low pressure negative glow helium discharges and to answer the two main questions: (i)Are the molecular ions present and do they play an important role in the self sustainment of low pressure negative glow helium discharges? (ii) How does the molecular ion to atomic ion density ratio change in the discharge with pressure? In order to answer these questions we investigate similar glow discharges ($pL = $ const., $j/p^2 = $const.) in the 2-60 mbar pressure range. Four different discharges are studied at the conditions which correspond to the same $pL = 6$ mbar cm and reduced current density $j/p^2 = 0.027$ mA cm^{-2} mbar^{-2}: (i) $p = 2$ mbar, $j = 0.108$ mA cm^{-2}, $L = 3$ cm (ii) $p = 6$ mbar, $j = 0.972$ mA cm^{-2}, $L = 1$ cm, (iii) $p = 20$ mbar, $j = 10.8$ mA cm^{-2}, $L = 0.3$ cm and (iv) $p = 60$ mbar, $j = 97.2$ mA cm^{-2}, $L = 0.1$ cm.

The discharges are described by a one-dimensional hybrid model which combines a fluid model for atomic and molecular ions and slow electrons, the Monte Carlo (MC)

simulation of fast electrons, and a diffusion-reaction model of the metastable species (it has been found from the literature that the metastables play on important role in the formation of the atomic and molecular ions). In the simulation the fluid, Monte Carlo and metastable models are solved in an iterative way until the stationary state of the discharge is reached. The structure of the hybrid model and the transfer of physical quantities between the three submodels are presented on the flowchart shown in Fig. 1. The elementary processes taken into account in the model are summarized in Table 1 (for a more detailed discussion see Ref. (Kutasi et al., 2001).) For fast electrons we take into account elastic scattering (p1), excitation to metastable and several higher excited states (up to $n = 5$) (p2-p3) as well as ionization (p4). The excited atoms (including the $n = 3$ to $n = 5$ states) can participate in associative ionization process (p5) in which molecular ions are created. The singlet and triplet atomic metastables may convert into triplet atomic and molecular metastables, respectively (p6-p7). The singlet atomic metastables also may convert to ground state atoms due to collision with the gas atoms (p8). The atomic and molecular ions are partly created in metastable-metastable associative ionization processes which result in the loss of metastables (p9). The metastables are also lost in deexcitation processes (p10-p11). The atomic ions convert into molecular ions through the ion conversion process (p12). The atomic ions are lost through collisional radiative (p13) and radiative recombination (p14). The molecular ions are lost through dissociative recombination (p15) (this process was not taken into account in the model of (Kutasi et al., 2001)), collisional radiative recombination (p16) and three body recombination (p17) processes.

Table 1: *Elementary processes considered in the model. He(S), He(T) and He(M) denote the singlet atomic, triplet atomic and molecular metastables, respectively.*

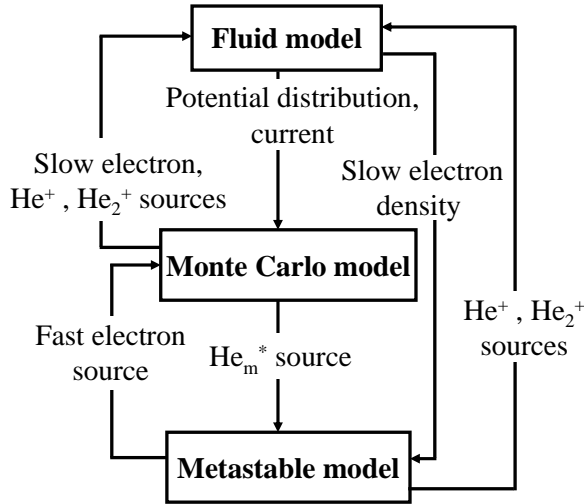| Proc. id.	Reaction Process	Proc. id.	Reaction Process
p1	$He+e^-\rightarrow He+e^-$	p10	$He(S)+e^-\rightarrow He+e^-$
p2	$He+e^-\rightarrow He(S,T)+e^-$	p11	$He(T)+e^-\rightarrow He+e^-$
p3	$He+e^-\rightarrow He^*+e^-$	p12	$He^++2He\rightarrow He_2^++He$
p4	$He+e^-\rightarrow He^++2e^-$	p13	$He^++2e^-\rightarrow He^*+e^-$
p5	$He^* + He \rightarrow He_2^+ + e^-$	p14	$He^++e^-\rightarrow He+h\nu$
p6	$He(S)+e^-\rightarrow He(T)+e^-$	p15	$He_2^++e\rightarrow He(1^1S)+He(2^3S)$
p7	$He(T)+2He\rightarrow He(M)+He$	p16	$He_2^++2e^-\rightarrow He_2^*+e^-$
p8	$He(S)+He\rightarrow 2He$	p17	$He_2^++e^-+He\rightarrow He_2^*+He$
p9	$He(S,T)+He(S,T)\rightarrow He^++He+e^-$		
	$He_2^++e^-$		

Figure 1: *Flowchart of the model.*

The input parameters of such a hybrid model are the discharge voltage, gas pressure, rate coefficients of different processes, the electron collisional cross sections, diffusion and mobility coefficients, the temperature of bulk (slow) electrons kT_e, and the secondary electron emission coefficient γ. One part of these parameters can be determined experimentally, the other part can be found in the literature, however there is a lack of data for the (i) electron temperature and (ii) secondary electron emission coefficient. Hybrid models of negative glow discharges conventionally use a constant characteristic energy for the slow electrons, which is chosen to be $kT_e = 1$ eV in almost all studies. In some previous investigations on low pressure negative glow discharges cold electron temperatures significantly lower than 1 eV have been found. These studies include laser based diagnostics of Den Hartog et al. (1989), theoretical calculations of Arslanbekov et al. (1998), Langmuir probe measurement of Bogaerts et al. (1995), Angstadt et al. (1993) and Ohsawa et al. (1991), Thomson scattering measurements of Gamez et al. (2004). In all of these works cold electron temperatures ranging between 0.08 and 0.5 eV have been found. Considering these data, the 1 eV value, used in most hybrid model-based simulations, may be too high. As the determination of the electron temperature in a wide pressure range is difficult in our work we also investigate the effect of the slow electron temperature on the discharge characteristics.

3.2   Results of the model

First the discharge characteristics calculated for 2 mbar pressure are presented. The model predicts the formation of cathode sheath - negative glow structure, see Fig. 2(a); the electric field falls nearly linearly from the cathode, and it is closely zero in the negative glow region. The charge density distributions - shown in Fig. 2(b) - indicate the presence of a quasi-neutral plasma in the negative glow and the dominance of the positive ions in the cathode sheath. According to the calculated charge fluxes Fig. 2(c) a part of the ions flows to the anode, which is the consequence of the small negative field present in the anode vicinity, due to the reversal of the electric field in the negative glow, see Fig. 2(d). The modelling results show that the position of the field reversal coincides with the position of the maximum density.
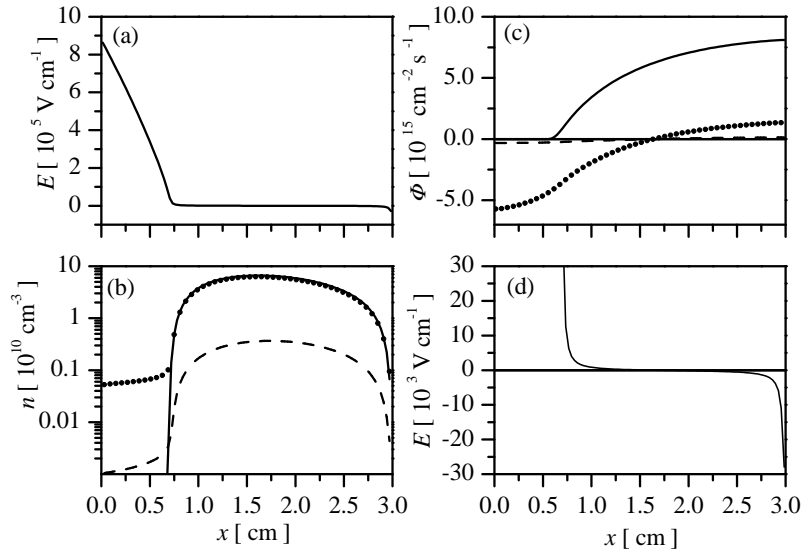
Figure 2: *(a) Axial distribution of the electric field; (b) Density distribution of the slow electrons (—), atomic (•) and molecular (– – –) ions; (b) Flux of the slow electrons (—), atomic (•) and molecular (– – –) ions; (d) Axial distribution of the electric field enlarged for the negative glow.*

The dependence of calculated discharge characteristics on the assumed value of the electron temperature is studied in details in the forthcoming part of the paper. First the dependence of the current density on kT_e at different pressures is studied. The results are illustrated in Fig. 3: the current density increases with increasing electron temperature. The results show that in order to obtain by modelling the experimental

current density the electron temperature in the discharges of 2-60 mbar pressure have to be chosen in the 0.1 - 0.3 eV range. Assuming higher kT_e values in the hybrid models the current density can be strongly overestimated. At low pressures assuming an electron temperature of 1 eV introduces a 20% error in the current density, however with increasing pressure this error raises and at 60 mbar reaches 60%. This strong dependence of the current densities on the electron temperature let us conclude that for correct modelling the accurate determination of the electron temperature is required.
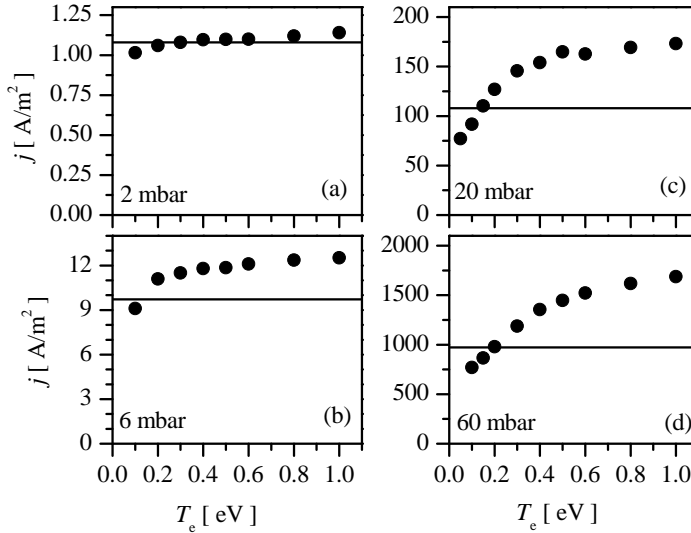
Figure 3: *Calculated current density (•) as a function of the assumed electron temperature at different gas pressures. The heavy horizontal lines in the panels represent the experimental current density at U = 350 V.*

In the following the percentage of molecular ions in the negative glow as a function of the assumed kT_e is studied and presented in Fig. 4(a). The percentage of molecular ions decreases with increasing electron temperature, in comparison with the 0.1 eV case, at 1 eV the percentage of molecular ions decreases by about 10% at $p = 60$ mbar. The results show that in the 0.1-0.2 eV range, the percentage of molecular ions decreases by about 5% in the case of 2, 6 and 20 mbar, while at 60 mbar increases by about 2%. In the case of $kT_e = 0.2$ eV - which is supposed by us to be a realistic value for the electron temperature - at 2 mbar 6% of ions are molecular ions, at 6 mbar 16%, at 20 mbar 30% and at the highest pressure investigated 60 mbar 42%. In Fig. 4(b) the percentage of the ion current carried by molecular ions at the cathode as a func-
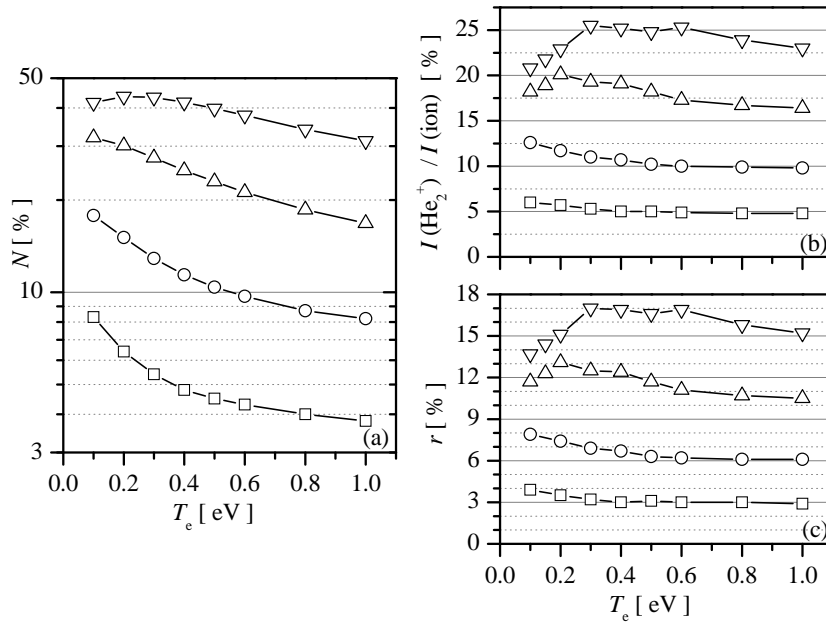
Figure 4: *(a) Percentage of molecular ions in the negative glow as a function of the assumed electron temperature at 2 mbar ($\square$), 6 mbar ($\bigcirc$), 20 mbar ($\triangle$), 60 mbar ($\triangledown$). (b) Percentage of the ion current carried by the molecular ions at the cathode and (c) percentage of secondary electrons released by molecular ions at the cathode as a function of the assumed electron temperature at 2 mbar ($\square$), 6 mbar ($\bigcirc$), 20 mbar ($\triangle$), 60 mbar ($\triangledown$).*

tion of the assumed electron temperature is presented. The ratio of the molecular ion current $I_{\mathrm{He}_2^+}$ to the total ion current shows a slight dependence on the electron temperature. In the case of $kT_e = 0.2$ eV at 2 mbar 5% of the ion current is carried by the molecular ions, at 6 mbar this percentage increases up to 12% and at 60 mbar reaches 22%. The self sustained mode of operation of the discharge is assured by the ions arriving at the cathode surface which induce the emission of secondary electrons. Fig. 4(c) shows the percentage of secondary electrons released by the molecular ions, $r = 100 \times \gamma_{\mathrm{He}_2^+} I_{\mathrm{He}_2^+} / (\gamma_{\mathrm{He}_2^+} I_{\mathrm{He}_2^+} + \gamma_{\mathrm{He}+} I_{\mathrm{He}+})$. At 2 mbar 3% of electrons are released by the molecular ions, at 6 mbar 7% and at 60 mbar 15%. These results give us an insight about the increasing importance of molecular ions in the self-sustainment of the discharge.

4 Summary

In the paper the hybrid model and the investigations carried out on a helium glow discharge in the 2-60 mbar pressure range have been presented. The calculations have been carried out for similar discharges (pL and j/p^2 const.) at a constant discharge voltage $V = 350$ V. Besides the role of molecular ions in the discharge the effect of the electron temperature on discharge characteristics have been investigated. The model have shown that even at low pressures like 6 mbar 16% of ions are molecular ions and they play on important role in the secondary electron emission. The comparison of the measured and calculated current densities indicated that the electron temperature in the 2-60 mbar pressure domain is in the 0.1-0.3 eV range, which is significantly lower than the $kT_e = 1$ eV value conventionally used in hybrid models. We have shown that by assuming $kT_e = 1$ eV – as the majority of hybrid models do – the current density of the discharges can be significantly overestimated.

From our investigations we conclude that for correct modelling the accurate experimental determination of electron temperature is necessary and in the case of helium discharges even at low pressures the presence of molecular ions should be taken into account.

Acknowledgement

References

Surendra, M., D. B. Graves, G. M. Jellum 1990, Phys. Rev. A, 41, 1112

Fiala, A., Pitchford, L. C., Boeuf, J. P. 1994, Phys. Rev. E, 49, 5607

Donkó, Z. 1998, Phys. Rev. E, 57, 7126

Boeuf, J. P., Marode, E. 1982, J.Phys. D: Appl. Phys., 15, 2169

Ichikawa, Y., Teii, S. 1980, J. Phys. D: Appl. Phys., 13, 2031

Kutasi, K., Hartmann, P., Donkó, Z. 2001, J. Phys. D: Appl. Phys., 34, 3368

Den Hartog, E. A., O'Brian, T. R., Lawler, J. E. 1989, Phys. Rev. Lett., 62, 1500

Arslanbekov, R. R., Kudryavtsev, A. A. 1998, Phys. Rev. E, 58, 6539

Bogaerts, A., Quentmeier, A., Jakubowski, N., Gijbels, R. 1995, Spectrochim. Acta B, 50, 1337

Angstadt, A. D., Whelan, J., Hess, K. R. 1993, Microchem. J., 47, 206

Ohsawa, A., Ohuchi, M., Kubota, T. 1991, Meas. Sci. Technol., 2, 801

Gamez, G., Bogaerts, A., Andrade, F., Hieftje 2004, Spectrochim. Acta B, 59, 435